

# On Fresnel-Airy Equations, Fabry-Perot Resonances and Surface Electromagnetic Waves in Arbitrary Bianisotropic Metamaterials

Maxim Durach\*, Felix Williamson, Jacob Adams, Tonilynn Holtz, Pooja Bhatt, Rebecka Moreno, and Franchesca Smith

**Abstract**—We introduce a theory of optical responses of bianisotropic layers with arbitrary effective medium parameters, which results in generalized Fresnel-Airy equations for reflection and transmission coefficients at all incidence directions and polarizations. The poles of these equations provide explicit expressions for the dispersion of Fabry-Perot resonances and surface electromagnetic waves in bianisotropic layers and interfaces. The existence conditions of these resonances are topologically related to the zeros of the high- $k$  characteristic function  $h(\mathbf{k}) = 0$  of bulk bianisotropic materials and taxonomy of bianisotropic media according to the hyperbolic topological classes [32, 33].

## 1. INTRODUCTION

The studies of bianisotropic optical materials (bianisotropics [1–3]) emerged [4–7] from the investigations of magnetoelectric effects in moving media first observed by Roentgen and Wilson [4, 8–10] and from consideration of magnetoelectric crystals started by Landau, Lifshitz, and Dzyaloshinskii [11–15]. Through the machinery of transformational optics [16–18], it has been demonstrated that light propagation through bianisotropic optical metamaterials can serve as simulations of Universe-aged cosmology problems from times immemorial [19, 20]. Now bianisotropic materials attract a lot of attention due to the practical development of complex anisotropic and bianisotropic photonic metamaterials in a wide range of frequency bands [21, 22]. Metamaterial structures feature many exotic optical properties important for applications, such as superresolution imaging and sensing, optical cloaking, subwavelength optical confinement and guiding, emission rate and directivity control, optical magnetism etc. [21–24]. Typically, these properties depend on metamaterials being anisotropic and bianisotropic optical media [21, 22].

Bianisotropic media are the most general case of local linear media [3–7, 25] and are characterized by the effective material parameters grouped into a  $6 \times 6$  material parameters matrix  $\hat{M}$ , which relate the electric displacement field  $\mathbf{D}$  and magnetic field  $\mathbf{B}$  with fields  $\mathbf{E}$  and  $\mathbf{H}$ :

$$\begin{pmatrix} \mathbf{D} \\ \mathbf{B} \end{pmatrix} = \hat{M} \begin{pmatrix} \mathbf{E} \\ \mathbf{H} \end{pmatrix} = \begin{pmatrix} \hat{\epsilon} & \hat{X} \\ \hat{Y} & \hat{\mu} \end{pmatrix} \begin{pmatrix} \mathbf{E} \\ \mathbf{H} \end{pmatrix}. \quad (1)$$

The  $3 \times 3$  matrices  $\hat{\epsilon}\hat{\mu}\hat{X}\hat{Y}$  are dielectric permittivity, magnetic permeability, and two magnetoelectric coupling matrices, respectively. Until recently very few general concrete properties of bulk bianisotropic media were established beyond formulaic apparatus due to the complexity of these materials and multiparametric nature of these media [3, 25–27]. Bulk bianisotropic materials feature quartic isofrequency Fresnel wave surfaces [28–31] which can be described using the direction-dependent index of refraction operator theory [32, 33]. Note that, unlike quadric and cubic surfaces, quartic surfaces

Received 7 February 2022, Accepted 3 March 2022, Scheduled 9 March 2022

\* Corresponding author: Maxim Durach (mdurach@georgiasouthern.edu).

The authors are with the Department of Physics and Astronomy, Georgia Southern University, Statesboro, Georgia 30461, USA.

have not been completely explored and fully classified in mathematical sciences [34, 35]. In 2020 Durach et al. proposed a taxonomy of bianisotropic optical media based on the number of double cones that isofrequency Fresnel wave surfaces feature at high  $k$ -vectors [32, 33]. According to this taxonomy, both bianisotropic and anisotropic media can be classified by 5 topological classes non-, mono-, bi-, tri-, and tetrahyperbolic materials [32, 33, 36–40]. An example of a tetrahyperbolic isofrequency Fresnel wave surface is shown in Fig. 1(a) for the effective medium with matrix  $\hat{M}$  color coded in the bottom of that panel. Durach et al. taxonomy [32, 33] provide a framework for future advances not only in the field of bianisotropic metamaterials, but also for hyperbolic metamaterials, already known for applications in optical imaging, hyperlensing, and emission rate and directivity control utilizing the diverging optical density of high- $k$  states [22, 24, 39, 40].

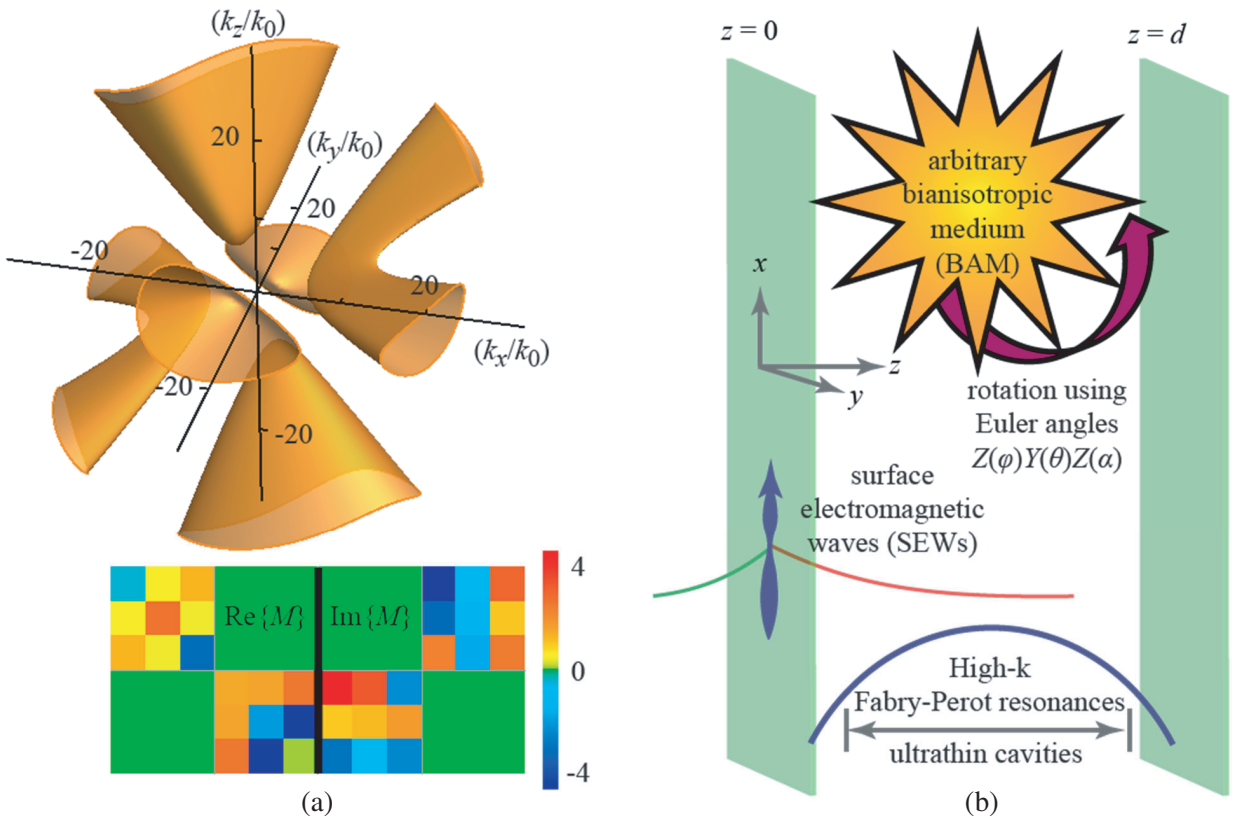


**Figure 1.** (a) Isofrequency Fresnel wave surface in  $k$ -space for a tetrahyperbolic bianisotropic material with  $\hat{M}$  matrix illustrated with color coding in the bottom of the panel. (b) Schematic illustrating the conventions in this paper as described in the text.

Researchers in bianisotropics are attempting to use the optical responses of specific bianisotropic metamaterial and metasurface structures including reflection, transmission, and scattering characteristics, resonances, surface electromagnetic waves (SEWs), and various properties of field distributions to retrieve the information about the effective material parameters [41–54] and the constituent meta-atoms [55–58]. Another important direction is to homogenize metamaterials composed of specific meta-atoms into an effective medium [59–75] or inversely to use structure synthesis or modular approach of materiatronics [76–81] to decompose the effective medium into constituent meta-atoms. At the same time, predicting and classifying the general features of the optical responses and electromagnetic fields in bianisotropic effective media is challenging and limited to special important cases [82–102], and has not been completed for a generic bianisotropic media due to the difficulty in explicit determination of the waves propagating and decaying in a particular direction in such a medium.

For example, obtaining Fresnel equations can be challenging at generic bianisotropic interfaces [103]. Another reason for the complications is the need to establish the additional boundary conditions (ABCs) in extreme non-reciprocal cases [104]. Even though a classification of individual SEWs at bianisotropic boundaries can be introduced based on propagation and penetration characteristics of the waves [105] and the invariance classes for individual SEWs with respect to variations of material parameters can be established [105], the classification of the isofrequency curves for SEWs is difficult to obtain [106–111].

In general, finding resonances and SEWs in stratified bianisotropic arrays represents a transcendental optics problem and their general properties have not been established previously in the literature [112–117]. The optical responses of an isotropic layer are described by Airy formulas [118, 119], whose poles correspond to the Fabry-Perot resonances [120, 121] and describe both guided and SEW modes of the layers [122, 123]. In isotropic materials and some bianisotropic materials, the electromagnetic fields are characterized by specific polarizations [124–128], but generally the anisotropic and bianisotropic layers and metasurfaces feature multimode resonances with coupled polarizations, which has been an additional complication [129–131].

In this paper we introduce a complete theory of optical responses of arbitrary bianisotropic planar cavities and wave guides. We obtain the explicit expressions for the reflection and transmission coefficients in any polarization from both sides of a generic bianisotropic layer, and an explicit expression which describes the Fabry-Perot resonances and surface electromagnetic waves propagating in such bianisotropic layers.

We relate the conditions for these resonances with the orientation of the bulk Fresnel wave surface with respect to the boundaries of the layer (see Fig. 1 for schematic). The regions where Fabry-Perot resonances may propagate are separated from the regions of surface electromagnetic waves by the zero curve of the high- $k$  characteristic function,  $h(\mathbf{k})$ , characterizing the topological phase of bulk bianisotropic materials according to Durach et al. taxonomy [32, 33].

We demonstrate that thin subwavelength layers form cavities supporting high- $k$  Fabry-Perot resonances if the bianisotropic material is oriented such that the high- $k$  direction, given by the zero of high- $k$  characteristic function, is close to perpendicular to the interfaces of the layer. The density of Fabry-Perot resonances diverges as the bianisotropic material direction approaches  $h(\mathbf{k}) = 0$ . As the thickness of the layer increases, the resonance spectrum becomes more populated with lower- $k$  modes of the bulk bianisotropic media. The SEWs appear as arcs in the regions where evanescent waves are supported between the regions with propagating waves. The resonances of the layer are represented as the interference of multiple channels of energy transfer through the cavity.

## 2. THEORY OF OPTICAL RESPONSE AND RESONANCES OF BIANISOTROPIC LAYERS

We base our theory of optical responses and resonances of bianisotropic layers on the characteristic matrix formalism [132, 33]. The explicit expression for the  $4 \times 4$  characteristic matrix of bianisotropic media  $\hat{\Delta}$  was recently obtained in terms of the material parameters contained within  $\hat{M}$  and the parallel to the layer component of the  $k$ -vector  $\mathbf{k}_{\parallel} = k_0(q_x q_y)$  [33]. For  $\mathbf{k}_{\parallel} = 0$  the characteristic matrix  $\hat{\Delta}$  corresponds to the index of refraction operator  $\hat{N}$  in the  $z$ -direction [32, 33]. The eigenvalues  $q_z^{(i)} = q_z^{(i)}(q_x, q_y)$ ,  $i = 1, \dots, 4$  of the characteristic matrix  $\hat{\Delta}$  provide the shape of the isofrequency Fresnel wave surface. Electromagnetic fields in a bianisotropic media can be expressed in terms of the eigenvalues  $q_z^{(i)}$  and eigenvectors  $\Gamma_{\parallel}^{(i)} = (E_x^{(i)}, E_y^{(i)}, H_x^{(i)}, H_y^{(i)})^T$  of the matrix  $\hat{\Delta}$  using eigenvalue decomposition

$$\hat{\Delta} = \hat{F} \cdot \hat{Q} \cdot \hat{F}^{-1} \quad (2)$$

where  $\hat{F} = (\Gamma_{\parallel}^{(1)}, \Gamma_{\parallel}^{(2)}, \Gamma_{\parallel}^{(3)}, \Gamma_{\parallel}^{(4)})$  is the eigenvector matrix composed of eigenvectors of matrix  $\hat{\Delta}$ , and  $\hat{Q} = \text{diag}\{q_z^{(1)}, q_z^{(2)}, q_z^{(3)}, q_z^{(4)}\}$ .

The  $z$ -dependence of the  $x$ - and  $y$ -components of the field can be expressed as

$$\begin{pmatrix} E_x \\ E_y \\ H_x \\ H_y \end{pmatrix} = \begin{pmatrix} \sum A_i E_x^{(i)} e^{ik_0 q_z^{(i)} z} \\ \sum A_i E_y^{(i)} e^{ik_0 q_z^{(i)} z} \\ \sum A_i H_x^{(i)} e^{ik_0 q_z^{(i)} z} \\ \sum A_i H_y^{(i)} e^{ik_0 q_z^{(i)} z} \end{pmatrix} = \hat{F} \cdot \exp\left(ik_0 \hat{Q} z\right) \cdot A \quad (3)$$

where the amplitude vector  $A = (A^{(1)}, A^{(2)}, A^{(3)}, A^{(4)})^T$  is composed of the amplitudes of the eigenmodes in Eq. (3).

For a wave with  $\mathbf{k}_{\parallel} = k_0(q_x, 0)$  in vacuum  $\hat{Q}_0 = \text{diag} q_z q_z, -q_z, -q_z$  is the eigenvalue matrix with  $q_z = \sqrt{1 - q_x^2}$ . Two sets of eigenvectors in vacuum  $\hat{F}_0 = (\Gamma_{\parallel}^{(1)}, \Gamma_{\parallel}^{(2)}, \Gamma_{\parallel}^{(3)}, \Gamma_{\parallel}^{(4)})$  are typically introduced. First, for linear polarization we use

$$\Gamma_{\parallel, \text{TM}}^{(1)} = \begin{pmatrix} E_x \\ E_y \\ H_x \\ H_y \end{pmatrix} = \begin{pmatrix} q_z \\ 0 \\ 0 \\ 1 \end{pmatrix} \Gamma_{\parallel, \text{TE}}^{(2)} = \begin{pmatrix} 0 \\ 1 \\ -q_z \\ 0 \end{pmatrix} \Gamma_{\parallel, \text{TM}}^{(3)} = \begin{pmatrix} -q_z \\ 0 \\ 0 \\ 1 \end{pmatrix} \Gamma_{\parallel, \text{TE}}^{(4)} = \begin{pmatrix} 0 \\ 1 \\ q_z \\ 0 \end{pmatrix} \quad (4)$$

Secondly, the left- and right-circularly polarized eigenvectors  $\Gamma_{\parallel, L, R}^{(i)}$  are

$$\Gamma_{\parallel, L}^{(1)} = \Gamma_{\parallel, \text{TM}}^{(1)} + i\Gamma_{\parallel, \text{TE}}^{(2)} \Gamma_{\parallel, R}^{(2)} = \Gamma_{\parallel, \text{TE}}^{(2)} + i\Gamma_{\parallel, \text{TM}}^{(1)} \quad (5a)$$

$$\Gamma_{\parallel, L}^{(3)} = \Gamma_{\parallel, \text{TM}}^{(3)} + i\Gamma_{\parallel, \text{TE}}^{(4)} \Gamma_{\parallel, R}^{(4)} = \Gamma_{\parallel, \text{TE}}^{(4)} + i\Gamma_{\parallel, \text{TM}}^{(3)} \quad (5b)$$

We consider a bianisotropic layer placed into the vacuum at  $0 < z < d$  (Fig. 1(b)). First, consider the incidence from the  $z < 0$  side of TM, or left-handed circular polarized  $\Gamma_{\parallel}^{(1)}$  waves depending on the basis eigenvectors chosen (Eqs. (4)–(5)). The  $z$ -dependence of the fields  $V_{-}(z)$  in the vacuum at  $z < 0$  is

$$V_{-}(z) = \Gamma_{\parallel}^{(1)} e^{ik_z z} + \left(r_{13}\Gamma_{\parallel}^{(3)} + r_{14}\Gamma_{\parallel}^{(4)}\right) e^{-ik_z z} \quad (6)$$

where  $k_z = k_0 q_z$ . On the other side of the layer at  $z > d$

$$V_{+}(z) = \left(t_{11}\Gamma_{\parallel}^{(1)} + t_{12}\Gamma_{\parallel}^{(2)}\right) e^{ik_z(z-d)} \quad (7)$$

Similarly, the functions  $V_{-}(z)$  and  $V_{+}(z)$  can be written for TM and TE (or left- and right-handed) polarization incidence from both sides of the bianisotropic layer, with different reflection and transmission coefficients  $r_{ab}t_{ab}$ , where  $a = 1, \dots, 4$  corresponds to the number of incidence wave and  $b = 1, \dots, 4$  denotes the number of the reflection or transmission wave in the desired basis. We denote the eigenvalues and eigenvectors in the bianisotropic layer as  $\hat{Q}_B = \text{diag}\{q_z^{(1)}, q_z^{(2)}, q_z^{(3)}, q_z^{(4)}\}$  and  $\hat{F}_B = (\Gamma_{\parallel, B}^{(1)}, \Gamma_{\parallel, B}^{(2)}, \Gamma_{\parallel, B}^{(3)}, \Gamma_{\parallel, B}^{(4)})$ , respectively. The amplitudes for the fields in the bianisotropic layer Eq. (3) are denoted as  $A_a$  and grouped into vector  $A$ , where the subscript “ $a$ ” depends on the incidence wave (see Eq. (3)). For all types of incidence, the boundary conditions can be written as

$$V_{-}(0) = \hat{F}_B \cdot A \quad (8)$$

$$\hat{F}_B \cdot \exp\left(ik_0 d \hat{Q}\right) \cdot A = V_{+}(d) \quad (9)$$

The fields to the right and to the left of the layer can be related using Eqs. (8)–(9) and the coefficients  $A$  can be obtained as

$$V_{+}(d) = \hat{F}_B \cdot \exp\left(ik_0 d \hat{Q}\right) \cdot \hat{F}_B^{-1} \cdot V_{-}(0) = \exp\left(ik_0 d \hat{\Delta}\right) \cdot V_{-}(0) \quad (10)$$

$$A = \hat{F}_B^{-1} \cdot V_{-}(0) \quad (11)$$

Equation (10) can be written for all 4 types of excitation simultaneously in the matrix form

$$\hat{F}_{0-} + \hat{F}_{0+} \cdot R = \exp\left(ik_0d\hat{\Delta}\right) \cdot (\hat{F}_{0+} + \hat{F}_{0-} \cdot R) \quad (12)$$

using the *optical response matrix*  $\hat{R}$

$$\hat{R} = \begin{pmatrix} t_{11} & t_{21} & r_{31} & r_{41} \\ t_{12} & t_{22} & r_{32} & r_{42} \\ r_{13} & r_{23} & t_{33} & t_{43} \\ r_{14} & r_{24} & t_{34} & t_{44} \end{pmatrix} \quad (13)$$

where we group the waves with positive  $S_z > 0$  and negative  $S_z < 0$   $z$ -components of the Poynting vector into matrices  $\hat{F}_{0+}$  and  $\hat{F}_{0-}$ , respectively

$$\hat{F}_{0+} = \left(\Gamma_{\parallel}^{(1)}, \Gamma_{\parallel}^{(2)}, 0, 0\right), \quad \hat{F}_{0-} = \left(0, 0, \Gamma_{\parallel}^{(3)}, \Gamma_{\parallel}^{(4)}\right) \quad (14)$$

From Eq. (12) we provide the formal solution to the problem of finding the response matrix  $\hat{R}$  of an arbitrary bianisotropic layer

$$\hat{R} = \left(\hat{F}_{0+} - \exp\left(ik_0d\hat{\Delta}\right) \cdot \hat{F}_{0-}\right)^{-1} \left(\exp\left(ik_0d\hat{\Delta}\right) \cdot \hat{F}_{0+} - \hat{F}_{0-}\right) \quad (15)$$

which is composed of all possible reflection and transmission coefficients  $r_{ab}t_{ab}$ . Our result Eq. (15) generalizes the Airy formula for isotropic layers [118, 119] to arbitrary bianisotropic media. The poles of Eq. (15) describe Fabry-Perot resonances and surface electromagnetic waves in bianisotropic media as described below.

Note that the response matrix in the form  $\hat{R} = \hat{1} \cdot e^{ik_zd}$  corresponds to the complete invisibility (nihility) of the layer in both amplitude and phase in all polarizations, while deviations from the identity matrix in the response matrix corresponds to presence of forward or backward scattering [133]. Comparing Eqs. (5) and (10)–(15) for linear and circular polarizations we see that response matrices in linear and circular polarization are related as

$$R_{circ} = \left(1 + i\hat{B}\right)^{-1} R_{lin} \left(1 + i\hat{B}\right), \quad \hat{B} = \begin{pmatrix} 0 & 1 & 0 & 0 \\ 1 & 0 & 0 & 0 \\ 0 & 0 & 0 & 1 \\ 0 & 0 & 1 & 0 \end{pmatrix}$$

The formalism of the optical response matrix  $\hat{R}$  can be used for the design of novel bianisotropic planar optical components, such as cavities [130] or wave-plates [131]. Below we investigate Fabry-Perot resonances and surface electromagnetic waves using this formalism. The general condition for Fabry-Perot resonances and SEWs in bianisotropic media can be found as poles of the generalized Airy formula given by Eq. (15), or equivalently as zeros of the denominators  $\delta_A$ :

$$\delta_A = \det \left\{ \hat{F}_{0+} - \exp\left(ik_0d\hat{\Delta}\right) \cdot \hat{F}_{0-} \right\} \quad (16)$$

After tedious algebra Eq. (16) can be rewritten as

$$\delta_A = \left(D_{12}^- D_{34}^+ e^{i\varphi_{12}} + D_{13}^- D_{24}^+ e^{i\varphi_{13}} + D_{14}^- D_{23}^+ e^{i\varphi_{14}} + D_{23}^- D_{14}^+ e^{i\varphi_{23}} + D_{24}^- D_{13}^+ e^{i\varphi_{24}} + D_{34}^- D_{12}^+ e^{i\varphi_{34}}\right) / D_B \quad (17)$$

where  $\varphi_{ij} = ik_0(q_z^{(i)} + q_z^{(j)})d$ ,  $D_{ij}^- = \det(\Gamma_{\parallel}^{(1)}, \Gamma_{\parallel}^{(2)}, -\Gamma_{\parallel,B}^{(i)}, -\Gamma_{\parallel,B}^{(j)})$ , and  $D_{pq}^+ = \det(\Gamma_{\parallel,B}^{(p)}, \Gamma_{\parallel,B}^{(q)}, -\Gamma_{\parallel}^{(3)}, -\Gamma_{\parallel}^{(4)})$ ,  $D_B = \det(\hat{F}_B)$ .

### 3. OPTICAL RESPONSE OF BIANISOTROPIC LAYERS IN TERMS OF FRESNEL COEFFICIENTS AT BIANISOTROPIC SURFACES

To provide an insight into the physics of the resonance condition of Eqs. (16)–(17) we derive the Fresnel coefficients for a generic boundary of bianisotropic materials and express Eq. (15) in terms of these coefficients as is frequently done for isotropic layers. To accomplish this, we need to assume that there

are no additional waves on the boundary, otherwise additional boundary conditions (ABCs) introduced in Ref. [104] are needed. We assume that waves  $\Gamma_{\parallel,B}^{(1)}\Gamma_{\parallel,B}^{(2)}$  have positive  $S_z > 0$  and  $\Gamma_{\parallel,B}^{(3)}\Gamma_{\parallel,B}^{(4)}$  have negative  $S_z < 0$ . Considering the incidence of  $\Gamma_{\parallel,B}^{(1)}\Gamma_{\parallel,B}^{(2)}$  from the  $z < 0$  side the Fresnel coefficients  $r_{ab}^F t_{ab}^F$  can be obtained from boundary conditions [104, 105] and are given by

$$\begin{pmatrix} \hat{T}_{12} \\ \hat{R}_{12} \end{pmatrix} = \left( \Gamma_{\parallel}^{(1)}, \Gamma_{\parallel}^{(2)}, -\Gamma_{\parallel,B}^{(3)}, -\Gamma_{\parallel,B}^{(4)} \right)^{-1} \cdot \left( \Gamma_{\parallel,B}^{(1)}, \Gamma_{\parallel,B}^{(2)} \right) \quad (18)$$

For the incidence of  $\Gamma_{\parallel,B}^{(3)}\Gamma_{\parallel,B}^{(4)}$  from the  $z > d$  side, the Fresnel coefficients are found from

$$\begin{pmatrix} \hat{T}_{34} \\ \hat{R}_{34} \end{pmatrix} = \left( \Gamma_{\parallel}^{(3)}, \Gamma_{\parallel}^{(4)}, -\Gamma_{\parallel,B}^{(1)}, -\Gamma_{\parallel,B}^{(2)} \right)^{-1} \cdot \left( \Gamma_{\parallel,B}^{(3)}, \Gamma_{\parallel,B}^{(4)} \right) \quad (19)$$

and  $\hat{T}_{12} = \begin{pmatrix} t_{11}^F & t_{21}^F \\ t_{12}^F & t_{22}^F \end{pmatrix} \hat{R}_{12} = \begin{pmatrix} r_{13}^F & r_{23}^F \\ r_{14}^F & r_{24}^F \end{pmatrix}$ ,  $\hat{T}_{34} = \begin{pmatrix} t_{33}^F & t_{43}^F \\ t_{34}^F & t_{44}^F \end{pmatrix} \hat{R}_{34} = \begin{pmatrix} r_{31}^F & r_{41}^F \\ r_{32}^F & r_{42}^F \end{pmatrix}$ , where  $r_{ab}^F t_{ab}^F$  are Fresnel reflection and transmission coefficients into eigenmode  $b$  upon incidence of eigenmode  $a$ . The boundary conditions Eqs. (18)–(19) can be combined into a single matrix equation

$$\hat{F}_B^{-1} \cdot \hat{F}_0 = \begin{pmatrix} \hat{1} & \hat{R}_{34} \\ \hat{R}_{12} & \hat{1} \end{pmatrix} \cdot \begin{pmatrix} \hat{T}_{12} & \hat{0} \\ \hat{0} & \hat{T}_{34} \end{pmatrix}^{-1} = \begin{pmatrix} \hat{T}_{12}^{-1} & \hat{R}_{34} \hat{T}_{34}^{-1} \\ \hat{R}_{12} \hat{T}_{12}^{-1} & \hat{T}_{34}^{-1} \end{pmatrix} \quad (20)$$

Using Eq. (20) we can rewrite the optical response matrix  $\hat{R}$  of a bianisotropic layer Eq. (15) in terms of Fresnel coefficients. First, let us express the characteristic matrix  $\hat{\Delta}$  using eigenvalue decomposition (Eq. (2)):  $\exp(ik_0 d \hat{\Delta}) = \hat{F}_B \cdot \exp(ik_0 d \hat{Q}) \cdot \hat{F}_B^{-1}$ . From this Eq. (15) can be expressed through matrix  $\hat{F}_B^{-1} \cdot \hat{F}_0$

$$\hat{R} = \left( \hat{F}_B^{-1} \hat{F}_{0+} - \exp(ik_0 d \hat{Q}) \hat{F}_B^{-1} \hat{F}_{0-} \right)^{-1} \left( \exp(ik_0 d \hat{Q}) \hat{F}_B^{-1} \hat{F}_{0+} - \hat{F}_B^{-1} \hat{F}_{0-} \right) \quad (21)$$

We introduce matrices

$$\hat{U}_+ = \hat{F}_B^{-1} \cdot \hat{F}_{0+} = \begin{pmatrix} \hat{T}_{12}^{-1} & \hat{0} \\ \hat{R}_{12} \hat{T}_{12}^{-1} & \hat{0} \end{pmatrix}, \quad \hat{U}_- = \hat{F}_B^{-1} \cdot \hat{F}_{0-} = \begin{pmatrix} \hat{0} & \hat{R}_{34} \hat{T}_{34}^{-1} \\ \hat{0} & \hat{T}_{34}^{-1} \end{pmatrix} \quad (22)$$

Substituting Eqs. (20) and (22) into Eq. (21) we express the optical response of the layer in terms of Fresnel coefficients at the boundaries of the layer in direct analogy to the Airy-Fresnel formula for isotropic layers

$$\hat{R} = \left( \hat{U}_+ - \exp(ik_0 d \hat{Q}) \cdot \hat{U}_- \right)^{-1} \left( \exp(ik_0 d \hat{Q}) \cdot \hat{U}_+ - \hat{U}_- \right) \quad (23)$$

Using Eqs. (18)–(23) we express the resonance denominators Eqs. (16)–(17) in terms of Fresnel coefficients as

$$\begin{aligned} \delta_A = & 1 - r_{13}^F r_{31}^F e^{i\phi_{13}} - r_{14}^F r_{41}^F e^{i\phi_{14}} - r_{23}^F r_{32}^F e^{i\phi_{23}} - r_{24}^F r_{42}^F e^{i\phi_{24}} \\ & + e^{i\phi_{13}} e^{i\phi_{24}} (r_{13}^F r_{31}^F r_{24}^F r_{42}^F - r_{13}^F r_{32}^F r_{24}^F r_{41}^F + r_{14}^F r_{41}^F r_{23}^F r_{32}^F - r_{14}^F r_{42}^F r_{23}^F r_{31}^F) \end{aligned} \quad (24)$$

where  $\phi_{pq} = k_0(q_z^{(p)} - q_z^{(q)})d$ .

Equation (24) provides the physical background for resonances of bianisotropic layers. As can be seen in general all 4 eigenmodes for a specific  $\mathbf{k}_{\parallel}$ , corresponding to propagating waves of the bulk materials with  $\mathbf{k} = (\mathbf{k}_{\parallel}, q_z^{(p)})$ , participate in the resonances. The resonances, as can be seen from Eq. (24), can be understood as interference of 4 propagation channels, which are related to single roundtrip phasors  $r_{pq}^F r_{qp}^F e^{i\phi_{pq}}$  involving (a) propagation in mode  $p$  across the layer, (b) reflection from mode  $p$  into mode  $q$ , (c) propagation in mode  $q$  backwards, and (d) reflection from mode  $q$  into mode  $p$  at the original interface. Additionally, the phasors corresponding to two roundtrips across the layer participate in the interference as the last term of Eq. (23). This equation generalizes the result obtained for cavities formed by two uniaxial metasurfaces described in Eq. (7) of Ref. [130].

#### 4. HIGH-K FABRY-PEROT RESONANCES IN THIN SUBWAVELENGTH BIANISOTROPIC CAVITIES

In Fig. 2(a) we plot the resonant denominator  $\delta_A$  in logarithmic scale for the bianisotropic material illustrated in Fig. 1(a). To emphasize that our method is applicable to arbitrary bianisotropic materials, the effective parameters matrix  $\hat{M}$  color-coded in the bottom of panel Fig. 1(a) corresponds to a reciprocal material with effective parameters randomly generated in the range between  $-5$  to  $5$ . This material features anisotropic dielectric permittivity, magnetic permeability, and chirality tensors, which can be engineered by combining split-ring, helix, omega, fishnet, parallel-plate, and wire meta-atoms [21, 22].

The dependence is shown on various orientations with respect to the boundaries of a subwavelength layer with  $(k_0d) = 0.1$  [see schematic in Fig. 1(b)]. The orientations are given using Euler angles in convention  $Z(\phi)Y(\theta)Z(\alpha)$ , i.e., the material is first rotated around  $z$ -axis by angle  $\alpha$ , then around  $y$ -axis by angle  $\theta$  and so on. The normal incidence  $\mathbf{k}_{\parallel} = 0$  is considered in Fig. 2. The orientations corresponding to the directions in which high- $k$  modes with  $k \rightarrow \infty$  propagate are given by the zeros of the *high- $k$  characteristic function*  $h(\mathbf{k}) = (\mathbf{k}^T \hat{\epsilon} \mathbf{k})(\mathbf{k}^T \hat{\mu} \mathbf{k}) - (\mathbf{k}^T \hat{X} \mathbf{k})(\mathbf{k}^T \hat{Y} \mathbf{k}) = 0$  introduced in [32, 33]. The orientations of bianisotropic medium such that the  $k \rightarrow \infty$  directions are perpendicular to the layer interfaces are indicated as red dashed curves in Fig. 2(a).

This curve separates the graph into regions with different number of eigenmodes with real  $q_z$  which is indicated by the red numbers. For each orientation, there are 4 eigenmodes whose  $q_z$  can be real or complex. In Fig. 2(a) the closed regions have 2 modes with real  $q_z$  and 2 with complex. The region in the space between the closed regions has 0 modes with real  $q_z$  and all 4 eigenmodes have complex  $q_z$ . The high- $k$  characteristic function  $h(\mathbf{k})$  is a bulk property related to the bulk Fresnel wave surface of the bianisotropic material (Fig. 1(a)). Since it serves as the separatrix between different sets of eigenmodes, the  $h(\mathbf{k})$  function establishes the topological bulk-edge correspondence between the waves in the bulk bianisotropic material and the guided waves of the bianisotropic cavities and interfaces.

For the formation of Fabry-Perot resonances the eigenmodes with real  $q_z$  are necessary, therefore, the Fabry-Perot resonances are only possible in the corresponding regions. In deeply subwavelength thin cavities, the high- $k$  Fabry-Perot resonances can be supported for the orientations with high- $k$  propagating modes close to the dashed red curves. This is seen by the dark resonance minima of  $\log_{10} \delta_A$  marked by red arrows in Fig. 2(a). A cross-section of Fig. 2(a) at  $\alpha = 1.8$  is shown in Fig. 2(b). One can see that zeros of  $h(\mathbf{k}) = 0$  correspond to the divergences  $\delta_A$ ; and for the orientations in the vicinity of these divergences one can find the high- $k$  Fabry-Perot resonances, as detailed in panels 2(c) and 2(d). In Fig. 2(c) the orientations corresponding to  $\alpha = 1.8$  and  $\theta = 0.835 \div 0.855$  are shown.

The  $n = 1, 2, 3, 12$  high- $k$  Fabry-Perot resonances corresponding to  $\lambda = nd/2$  modes are indicated by the red, green, blue, and purple dots, respectively. The field profiles for these modes are shown in panel 2(e). Note that close to the  $h(\mathbf{k}) = 0$  direction, the density of the Fabry-Perot resonances diverges as  $n \rightarrow \infty$ . A similar situation occurs for the orientations  $\alpha = 1.8$  and  $\theta = 1.815-1.845$ , demonstrated in Figs. 2(d) and 2(f). In these panels, the high- $k$  Fabry-Perot resonances with  $n = 1, 2, 3, 12$  are shown.

One can also see the diverging density of Fabry-Perot modes with  $n \rightarrow \infty$  close to the  $h(\mathbf{k}) = 0$  direction in the subwavelength bianisotropic cavity with  $(k_0d) = 0.1$ , investigated in Fig. 2.

#### 5. SURFACE ELECTROMAGNETIC WAVES IN BIANISOTROPIC MATERIALS

Surface electromagnetic waves at single anisotropic boundaries are known as Dyakonov surface waves or dyakonons [134–137]. This term has been extended to bianisotropic single boundaries in Ref. [138] and generic condition of their existence has been established as poles of Fresnel Eqs. (18) and (19), which represent the dispersion of SEWs at bianisotropic interfaces  $\det\{(\Gamma_{\parallel}^{(1)}, \Gamma_{\parallel}^{(2)}, -\Gamma_{\parallel,B}^{(3)}, -\Gamma_{\parallel,B}^{(4)})\} = 0$ ,  $\det\{(\Gamma_{\parallel}^{(3)}, \Gamma_{\parallel}^{(4)}, -\Gamma_{\parallel,B}^{(1)}, -\Gamma_{\parallel,B}^{(2)})\} = 0$  [138, 105].

The general condition for SEWs propagating along bianisotropic layers is given explicitly by Eqs. (16), (17), or (24). Consider the formation of SEWs in bianisotropic layers when all 4 eigenvectors  $\hat{Q}_B = \text{diag}\{q_z^{(1)}, q_z^{(2)}, q_z^{(3)}, q_z^{(4)}\}$  are to be complex. In this case the phase factors  $\phi_{pq} = k_0(q_z^{(p)} - q_z^{(q)})d = \phi'_{pq} + i\xi_{pq}$  become complex, and Eq. (24) provides the physical background for SEWs propagating

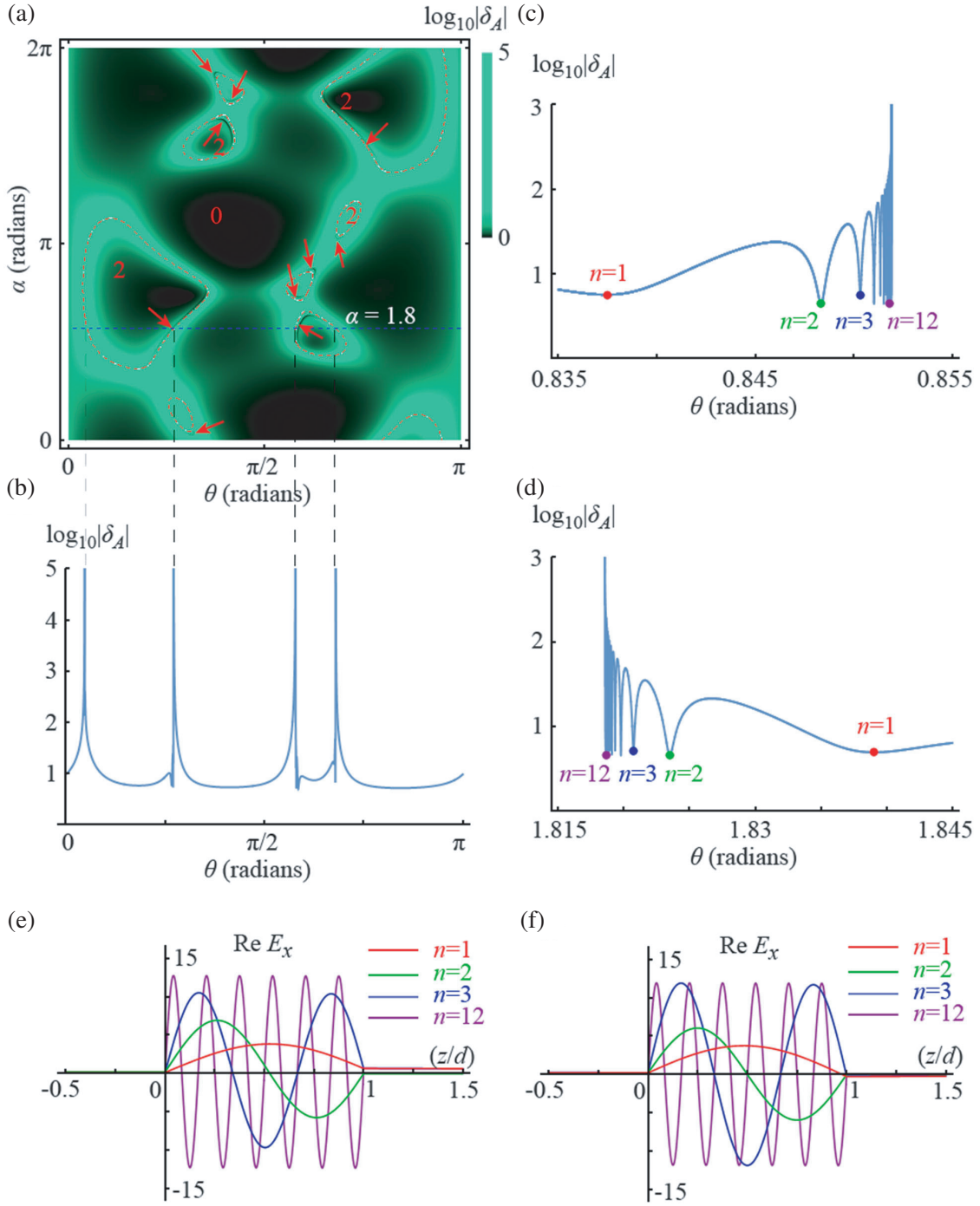


**Figure 2.** High- $k$  Fabry-Perot resonances in subwavelength bianisotropic cavity with  $(k_0d) = 0.1$  at normal incidence  $\mathbf{k}_{\parallel} = 0$ . (a) The resonant denominator  $\delta_A$  as a function of the bianisotropic material orientation with respect to the layer boundaries. (b) cross-section of panel (a) at  $\alpha = 1.8$ . (c) the same graph as (b) but magnified to illustrate the high- $k$  Fabry-Perot resonances corresponding to  $\lambda = nd/2$  modes with  $n = 1, 2, 3, 12$  in the range of  $\theta = 0.835 - 0.855$ . (d) the same graph as (b) but magnified to illustrate the high- $k$  Fabry-Perot resonances with  $n = 1, 2, 3, 12$  in the range of  $\theta = 1.815 - 1.845$ . (e) Field profiles of the high- $k$  Fabry-Perot resonances marked by dots in (c). (f) Field profiles of the high- $k$  Fabry-Perot resonances marked by dots in Fig. (d).



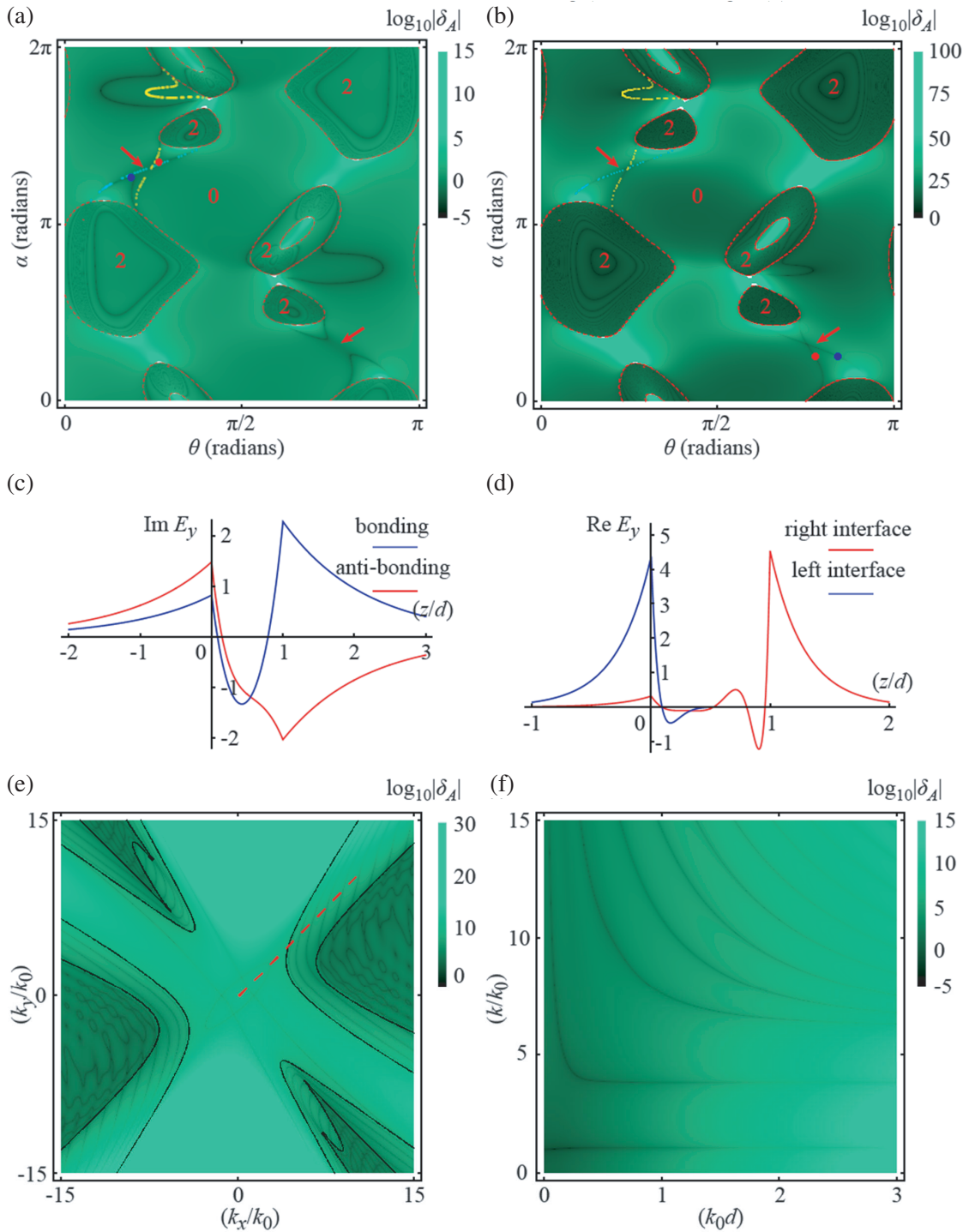


**Figure 3.** Surface electromagnetic waves in bianisotropic media. (a)–(b) The resonant denominator  $\delta_A$  as a function of the bianisotropic material orientation with respect to the layer boundaries for  $q_x = 2$  and  $(k_0d) = 0.5$  in (a) and  $(k_0d) = 2$  in (b); light blue and yellow outlines correspond to SEWs at individual boundaries of the layers. Panels (c)–(d) — Field profiles of SEWs for  $(k_0d) = 0.5$  in (c) and  $(k_0d) = 2$  in (d) for orientations indicated by blue and red dots in panels (a) and (b). Panel (e) — the isofrequency curves of SEWs in  $(k_x k_y)$  plane for  $(k_0d) = 2$ ,  $\theta = 1.4$ , and  $\alpha = 1.885$ . Panel (f) — dependence of the wave number of SEWs on layer thickness propagating in the direction indicated by red dashed in (e).

along bianisotropic layers. It shows that the 4 single roundtrip phasors  $r_{pq}^F r_{qp}^F e^{i\phi_{pq}}$  and the phasors corresponding to two roundtrips become exponentially smaller due to the factors  $e^{-\xi_{pq}}$  as the thickness of the layer is increased. At large thicknesses Eq. (24) is only fulfilled if one of the Fresnel coefficients  $r_{ab}^F$  diverges, which corresponds to a single boundary dyakonon [138, 105]. At finite thickness all phasors in Eq. (24) contribute to the SEW existence condition and their exponential factors  $e^{-\xi_{pq}}$  regulate the hybridization of SEWs at two interfaces of bianisotropic layers as we numerically demonstrate below.

In Fig. 3 we investigate the modes with longitudinal momentum  $q_x = 2$  in thicker layers for the same material as in Fig. 2, whose  $\hat{M}$  matrix is color-coded in the bottom of Fig. 1(a). Fig. 3(a) corresponds to  $(k_0d) = 0.5$ , while Fig. 3(b) to  $(k_0d) = 2$ . Due to the different longitudinal momentum the zero curve (red dashed) of the high- $k$  characteristic function  $h(\mathbf{k}) = 0$  separates Figs. 3(a)–(b) into somewhat different regions as compared to panel 2(a).

There are still 2 types of regions: (i) containing 2 modes with real  $q_z$  and 2 with complex  $q_z$  marked by the red number 2, and (ii) containing 0 modes with real  $q_z$  and all 4 eigenmodes with complex  $q_z$  marked by number 0. Note that due to larger thickness the layers in Fig. 3 support lower- $k$  Fabry-Perot resonances which populate most of the regions with real  $q_z$ , which can be seen as dark minima curves in these regions.

Surface electromagnetic waves also appear in the region with all evanescent waves as dark minima curves. For moderately thick layers with  $(k_0d) = 0.5$  [panels 3(a) and 3(c)], these SEWs feature hybridization and their fields are characterized by bonding (blue dot in Fig. 3(a) and blue curve in Fig. 3(c)) or anti-bonding behavior (red dot and red curve respectively) depending on the phases on the interfaces of the layer. Due to the hybridization coupling of the SEW fields at different interfaces, they feature anti-crossing in Fig. 3(a) as indicated by the red arrows. Because of this, the resonance conditions for hybridized modes deviate from the orientations at which SEWs of individual boundaries propagate, as outlined with yellow and blue curves for  $\theta < \frac{\pi}{2}$ . These outlines are found as poles of Fresnel Eqs. (18) and (19), which represent the dispersion of SEWs at bianisotropic interfaces  $\det\{\Gamma_{\parallel}^{(1)}, \Gamma_{\parallel}^{(2)}, -\Gamma_{\parallel,B}^{(3)}, -\Gamma_{\parallel,B}^{(4)}\} = 0$ ,  $\det\{\Gamma_{\parallel}^{(3)}, \Gamma_{\parallel}^{(4)}, -\Gamma_{\parallel,B}^{(1)}, -\Gamma_{\parallel,B}^{(2)}\} = 0$  [138, 105]. For  $\theta > \pi/2$  the existence conditions for these single boundary SEWs are symmetrically reflected in the  $\alpha < \pi$  region (not shown). In thick layers (see Fig. 3(b) and (d) for  $(k_0d) = 2$ ), the SEWs do not hybridize and localize at individual boundaries. The SEW resonance conditions shown in Fig. 3(b) perfectly follow the blue and yellow curves for single boundary SEWs localized at different boundaries. This can be seen from the field profiles shown in Fig. 3(d), where the blue curve corresponds to the blue dot in Fig. 3(b) and the red curve to the red dot, respectively.

In Fig. 3(e) we show an isofrequency  $k$ -curve for SEWs in the  $(k_x k_y)$  plane for  $\theta = 1.4$  and  $\alpha = 1.885$ , in a layer with thickness  $(k_0d) = 2$ . This graph features both elliptical and hyperbolic shapes of SEW isofrequency curves between the regions of guided waves in all 4 corners of this panel. We show the dependence of momentum of these modes on thickness in Fig. 3(f). This panel corresponds to the direction in the  $(k_x k_y)$  plane indicated by the red dashed line in Fig. 3(e). In Fig. 3(f) there are 2 SEW modes with  $k$  vectors depending on the thickness of the layer only for small thicknesses  $(k_0d) < 0.5$ , after which there is no hybridization in these SEWs. There are also 8 propagating modes in the upper right side of this panel.

## 6. CONCLUSION

To conclude, in this paper we presented a complete theory of optical responses of arbitrary bianisotropic media and found explicit conditions for Fabry-Perot resonances and surface electromagnetic waves in such structures. We topologically related the existence conditions of these resonances to the high- $k$  characteristic function of the bulk bianisotropic material and the taxonomy according to the hyperbolic topological classes.

## ACKNOWLEDGMENT

We acknowledge Georgia Southern University Scholarly Pursuit Funding Award, Summer Research Session Grant, Georgia Power Student Award, College Office of Undergraduate Research (COUR)

Grants from the College of Science and Mathematics at Georgia Southern University, and The Georgia Southern McNair Scholars Program.

## REFERENCES

1. Sihvola, A., I. Semchenko, and S. Khakhomov, "View on the history of electromagnetics of metamaterials: Evolution of the congress series of complex media," *Photonics and Nanostructures — Fundamentals and Applications*, Vol. 12, No. 4, 279–283, 2014.
2. Tretyakov, S. A., F. Bilotti, and A. Schuchinsky, "Metamaterials congress series: Origins and history," *2016 10th International Congress on Advanced Electromagnetic Materials in Microwaves and Optics (METAMATERIALS)*, 361–363, IEEE, 2016.
3. Mackay, T. G. and A. Lakhtakia, *Electromagnetic Anisotropy and Bianisotropy: A Field Guide*, World Scientific, 2010.
4. Cheng, D. K. and J. A. Kong, "Covariant descriptions of bianisotropic media," *Proceedings of the IEEE*, Vol. 56, No. 3, 248–251, 1968.
5. Cheng, D. K. and J. A. Kong, "Time-harmonic fields in source-free bianisotropic media," *Journal of Applied Physics*, Vol. 39, No. 12, 5792–5796, 1968.
6. Kong, J. A., *Electromagnetic Wave Theory*, Wiley-Interscience, 1990.
7. Lindell, I., A. Sihvola, S. Tretyakov, and A. J. Viitanen, *Electromagnetic Waves in Chiral and Bi-isotropic Media*, Artech House, 1994.
8. Röntgen, W. C., "Ueber die durch Bewegung eines im homogenen electrischen Felde befindlichen Dielectricums hervorgerufene electro-dynamische Kraft," *Annalen der Physik*, Vol. 271, No. 10, 264–270, 1888.
9. Wilson, H. A., "On the electric effect of rotating a dielectric in a magnetic field," *Philosophical Transactions of the Royal Society of London. Series A, Containing Papers of a Mathematical or Physical Character*, Vol. 204, Nos. 372–386, 121–137, 1905.
10. Chen, H. C., *Theory of Electromagnetic Waves: A Coordinate-free Approach*, McGraw-Hill, 1983.
11. Landau, L. D. and E. M. Lifshitz, *Electrodynamics of Continuous Media. Theoretical Physics*, Vol. 8, § 51, Fizmatlit, 2005.
12. Dzyaloshinskii, I. E., *J. Exp. Theoret. Phys.*, Vol. 37, 881, 1959 [translation: *Soviet Phys. — JETP*, Vol. 10, 628, 1960].
13. Astrov, D. N., *J. Exp. Theoret. Phys.*, Vol. 38, 984, 1960 [translation: *Soviet Phys. — JETP*, Vol. 11, 708, 1960].
14. Rado, G. T. and V. J. Folen, *Phys. Rev. Letters*, Vol. 7, 310, 1961.
15. Rado, G. T. and V. J. Folen, "Magnetolectric effects in antiferromagnetics," *Proceedings of the Seventh Conference on Magnetism and Magnetic Materials*, 1126–1132, Springer, 1962.
16. Pendry, J. B., D. Schurig, and D. R. Smith, "Controlling electromagnetic fields," *Science*, Vol. 312, No. 5781, 1780–1782, 2006.
17. Leonhardt, U., "Optical conformal mapping," *Science*, Vol. 312, No. 5781, 1777–1780, 2006.
18. Boston, S. R., "Time travel in transformation optics: Metamaterials with closed null geodesics," *Physical Review D*, Vol. 91, No. 12, 124035, 2015.
19. Mackay, T. G. and A. Lakhtakia, "Towards a metamaterial simulation of a spinning cosmic string," *Physics Letters A*, Vol. 374, No. 23, 2305–2308, 2010.
20. Smolyaninov, I. I. and E. E. Narimanov, "Metric signature transitions in optical metamaterials," *Physical Review Letters*, Vol. 105, No. 6, 067402, 2010.
21. Simovski, C. and S. Tretyakov, *An Introduction to Metamaterials and Nanophotonics*, Cambridge University Press, 2020.
22. Noginov, M. A. and V. A. Podolskiy (eds.), *Tutorials in Metamaterials*, CRC Press, 2011.
23. Engheta, N. and R. W. Ziolkowski (eds.), *Metamaterials: Physics and Engineering Explorations*, John Wiley & Sons, 2006.

24. Noginov, M. A., G. Dewar, M. W. McCall, and N. I. Zheludev, *Tutorials in Complex Photonic Media*, SPIE Press, 2009.
25. Tretyakov, S. A., “A personal view on the origins and developments of the metamaterial concept,” *Journal of Optics*, Vol. 19, No. 1, 013002, 2016.
26. Kong, J. A., “Theorems of bianisotropic media,” *Proceedings of the IEEE*, Vol. 60, No. 9, 1036–1046, 1972.
27. Berry, M., “The optical singularities of bianisotropic crystals,” *Proceedings of the Royal Society A: Mathematical, Physical and Engineering Sciences*, Vol. 461, No. 2059, 2071–2098, 2005.
28. Bateman, H., “Kummer’s quartic surface as a wave surface,” *Proceedings of the London Mathematical Society*, Vol. 2, No. 1, 375–382, 1910.
29. Baekler, P., A. Favaro, Y. Itin, and F. W. Hehl, “The Kummer tensor density in electrodynamics and in gravity,” *Annals of Physics*, Vol. 349, 297–324, 2014.
30. Favaro, A. and F. W. Hehl, “Light propagation in local and linear media: Fresnel-Kummer wave surfaces with 16 singular points,” *Physical Review A*, Vol. 93, No. 1, 013844, 2016.
31. Mulkey, T., J. Dillies, and M. Durach, “Inverse problem of quartic photonics,” *Optics Letters*, Vol. 43, No. 6, 1226–1229, 2018.
32. Durach, M., R. F. Williamson, M. Laballe, and T. Mulkey, “Tri- and tetrahyperbolic isofrequency topologies complete classification of bianisotropic materials,” *Applied Sciences*, Vol. 10, No. 3, 763, 2020.
33. Durach, M., “Tetra-hyperbolic and tri-hyperbolic optical phases in anisotropic metamaterials without magnetoelectric coupling due to hybridization of plasmonic and magnetic Bloch high- $k$  polaritons,” *Optics Communications*, Vol. 476, 126349, 2020.
34. Jessop, C. M., *Quartic Surfaces with Singular Points*, University Press, 1916.
35. Weisstein, E. W., *CRC Concise Encyclopedia of Mathematics*, CRC Press, 2003.
36. Kruk, S. S., J. W. Zi, E. Pshenay-Severin, K. O’Brien, D. N. Neshev, Y. S. Kivshar, and X. Zhang, “Magnetic hyperbolic optical metamaterials,” *Nature Commun.*, Vol. 7, No. 1, 1–7, 2016.
37. Tuz, V. R., I. V. Fedorin, and V. I. Fesenko, “Bi-hyperbolic isofrequency surface in a magnetic-semiconductor superlattice,” *Optics Letters*, Vol. 42, 4561, 2017.
38. Tuz, V. R. and V. I. Fesenko, “Magnetically induced topological transitions of hyperbolic dispersion in biaxial gyrotropic media,” *Journal of Applied Physics*, Vol. 128, 013107, 2020.
39. Guo, Z., H. Jiang, and H. Chen, “Hyperbolic metamaterials: From dispersion manipulation to applications,” *Journal of Applied Physics*, Vol. 127, No. 7, 071101, 2020.
40. Takayama, O. and A. V. Lavrinenko, “Optics with hyperbolic materials,” *JOSA B*, Vol. 36, No. 8, F38–F48, 2019.
41. Aladadi, Y. T. and M. A. Alkanhal, “Extraction of tensor parameters of general biaxial anisotropic materials,” *AIP Advances*, Vol. 10, No. 2, 025113, 2020.
42. Arslanagić, S., T. V. Hansen, N. A. Mortensen, A. H. Gregersen, O. Sigmund, R. W. Ziolkowski, and O. Breinbjerg, “A review of the scattering-parameter extraction method with clarification of ambiguity issues in relation to metamaterial homogenization,” *IEEE Antennas and Propagation Magazine*, Vol. 55, No. 2, 91–106, 2013.
43. Chen, L., Z.-Y. Lei, R. Yang, X.-W. Shi, and J. Zhang, “Determining the effective electromagnetic parameters of bianisotropic metamaterials with periodic structures,” *Progress In Electromagnetics Research*, Vol. 29, 79–93, 2013.
44. Chen, X., B.-I. Wu, J. A. Kong, and T. M. Grzegorzczuk, “Retrieval of the effective constitutive parameters of bianisotropic metamaterials,” *Physical Review E*, Vol. 71, No. 4, 046610, 2005.
45. Cheng, X., H. Chen, L. Ran, B.-I. Wu, T. M. Grzegorzczuk, and J. A. Kong, “Negative refraction and cross polarization effects in metamaterial realized with bianisotropic S-ring resonator,” *Physical Review B*, Vol. 76, No. 2, 024402, 2007.
46. Cohen, D. and R. Shavit, “Bi-anisotropic metamaterials effective constitutive parameters extraction using oblique incidence  $S$ -parameters method,” *IEEE Transactions on Antennas and Propagation*, Vol. 63, No. 5, 2071–2078, 2015.

47. Farahbakhsh, A., D. Zarifi, A. Abdolali, and M. Soleimani, "Technique for inversion of an inhomogeneous bianisotropic slab through an optimisation approach," *IET Microwaves, Antennas & Propagation*, Vol. 7, No. 6, 436–443, 2013.
48. Hasar, U. C., G. Buldu, Y. Kaya, and G. Ozturk, "Determination of effective constitutive parameters of inhomogeneous metamaterials with bianisotropy," *IEEE Transactions on Microwave Theory and Techniques*, Vol. 66, No. 8, 3734–3744, 2018.
49. Hasar, U. C., G. Ozturk, Y. Kaya, J. J. Barroso, and M. Ertugrul, "Simple and accurate electromagnetic characterization of omega-class bianisotropic metamaterials using the state transition matrix method," *IEEE Transactions on Antennas and Propagation*, Vol. 69, No. 10, 7064–7067, 2021.
50. Kraft, M., A. Braun, Y. Luo, S. A. Maier, and J. B. Pendry, "Bianisotropy and magnetism in plasmonic gratings," *ACS Photonics*, Vol. 3, No. 5, 764–769, 2016.
51. Kriegler, C. E., M. S. Rill, S. Linden, and M. Wegener, "Bianisotropic photonic metamaterials," *IEEE Journal of Selected Topics in Quantum Electronics*, Vol. 16, No. 2, 367–375, 2009.
52. Li, Z., K. Aydin, and E. Ozbay, "Determination of the effective constitutive parameters of bianisotropic metamaterials from reflection and transmission coefficients," *Physical review E*, Vol. 79, No. 2, 026610, 2009.
53. Odit, M., P. Kapitanova, P. Belov, R. Alaee, C. Rockstuhl, and Y. S. Kivshar, "Experimental realisation of all-dielectric bianisotropic metasurfaces," *Applied Physics Letters*, Vol. 108, No. 22, 221903, 2016.
54. Ozturk, G., U. C. Hasar, M. Bute, and M. Ertugrul, "Determination of constitutive parameters of strong-coupled bianisotropic metamaterials using oblique incidence scattering parameters," *IEEE Transactions on Antennas and Propagation*, Vol. 69, No. 2, 918–927, 2020.
55. Achouri, K., M. A. Salem, and C. Caloz, "General metasurface synthesis based on susceptibility tensors," *IEEE Transactions on Antennas and Propagation*, Vol. 63, No. 7, 2977–2991, 2015.
56. Lannebère, S., S. Campione, A. Aradian, M. Albani, and F. Capolino, "Artificial magnetism at terahertz frequencies from three-dimensional lattices of TiO<sub>2</sub> microspheres accounting for spatial dispersion and magnetoelectric coupling," *JOSA B*, Vol. 31, No. 5, 1078–1086, 2014.
57. Liu, X.-X. and A. Alù, "Generalized retrieval method for metamaterial constitutive parameters based on a physically driven homogenization approach," *Physical Review B*, Vol. 87, No. 23, 235136, 2013.
58. Liu, X.-X., Y. Zhao, and A. Alù, "Polarizability tensor retrieval for subwavelength particles of arbitrary shape," *IEEE Transactions on Antennas and Propagation*, Vol. 64, No. 6, 2301–2310, 2016.
59. Alaee, R., M. Albooyeh, M. Yazdi, N. Komjani, C. Simovski, F. Lederer, and C. Rockstuhl, "Magnetoelectric coupling in nonidentical plasmonic nanoparticles: Theory and applications," *Physical Review B*, Vol. 91, No. 11, 115119, 2015.
60. Albooyeh, M., S. Tretyakov, and C. Simovski, "Electromagnetic characterization of bianisotropic metasurfaces on refractive substrates: General theoretical framework," *Annalen der Physik*, Vol. 528, Nos. 9–10, 721–737, 2016.
61. Belov, P. A., C. R. Simovski, and S. A. Tretyakov, "Example of bianisotropic electromagnetic crystals: The spiral medium," *Physical Review E*, Vol. 67, No. 5, 056622, 2003.
62. Ciattoni, A. and C. Rizza, "Nonlocal homogenization theory in metamaterials: Effective electromagnetic spatial dispersion and artificial chirality," *Physical Review B*, Vol. 91, No. 18, 184207, 2015.
63. Fietz, C., "Electro-magnetostatic homogenization of bianisotropic metamaterials," *JOSA B*, Vol. 30, No. 7, 1937–1944, 2013.
64. Firestein, C. and R. Shavit, "Effective electrical parameters evaluation for non-dispersive metamaterials with highly interaction fields," *IET Microwaves, Antennas & Propagation*, Vol. 13, No. 8, 1151–1157, 2019.

65. Karamanos, T. D., S. D. Assimonis, A. I. Dimitriadis, and N. V. Kantartzis, “Effective parameter extraction of 3D metamaterial arrays via first-principles homogenization theory,” *Photonics and Nanostructures-Fundamentals and Applications*, Vol. 12, No. 4, 291–297, 2014.
66. Kildishev, A. V., J. D. Borneman, X. Ni, V. M. Shalaev, and V. P. Drachev, “Bianisotropic effective parameters of optical metamagnetics and negative-index materials,” *Proceedings of the IEEE*, Vol. 99, No. 10, 1691–1700, 2011.
67. Pors, A., I. Tsukerman, and S. I. Bozhevolnyi, “Effective constitutive parameters of plasmonic metamaterials: Homogenization by dual field interpolation,” *Physical Review E*, Vol. 84, No. 1, 016609, 2011.
68. Pors, A., M. Willatzen, O. Albrechtsen, and S. I. Bozhevolnyi, “Detuned electrical dipoles metamaterial with bianisotropic response,” *Physical Review B*, Vol. 83, No. 24, 245409, 2011.
69. Shaltout, A., V. Shalaev, and A. Kildishev, “Homogenization of bi-anisotropic metasurfaces,” *Optics Express*, Vol. 21, No. 19, 21941–21950, 2013.
70. Sihvola, A., “Olyslager approach to bianisotropic mixtures,” *2010 URSI International Symposium on Electromagnetic Theory*, IEEE, 2010.
71. Silveirinha, M. G., “Design of linear-to-circular polarization transformers made of long densely packed metallic helices,” *IEEE Transactions on Antennas and Propagation*, Vol. 56, No. 2, 390–401, 2008.
72. Simovski, C. and S. Tretyakov, “On effective electromagnetic parameters of artificial nanostructured magnetic materials,” *Photonics and Nanostructures — Fundamentals and Applications*, Vol. 8, No. 4, 254–263, 2010.
73. Simovski, C. R., E. Verney, S. Zouhdi, and A. Fourier-Lamer, “Homogenization of planar bianisotropic arrays on the dielectric interface,” *Electromagnetics*, Vol. 22, No. 3, 177–189, 2002.
74. Tsukerman, I., “Effective parameters of metamaterials: A rigorous homogenization theory via Whitney interpolation,” *JOSA B*, Vol. 28, No. 3, 577–586, 2011.
75. Wang, N. and G. P. Wang, “Effective medium theory with closed-form expressions for bi-anisotropic optical metamaterials,” *Optics Express*, Vol. 27, No. 17, 23739–23750, 2019.
76. Asadchy, V. S., A. Díaz-Rubio, and S. A. Tretyakov, “Bianisotropic metasurfaces: Physics and applications,” *Nanophotonics*, Vol. 7, No. 6, 1069–1094, 2018.
77. Asadchy, V. S. and S. A. Tretyakov, “Modular analysis of arbitrary dipolar scatterers,” *Physical Review Applied*, Vol. 12, No. 2, 024059, 2019.
78. Glybovski, S. B., S. A. Tretyakov, P. A. Belov, Y. S. Kivshar, and C. R. Simovski, “Metasurfaces: From microwaves to visible,” *Physics Reports*, Vol. 634, 1–72, 2016.
79. Mirmoosa, M. S., Y. Ra’di, V. S. Asadchy, C. R. Simovski, and S. A. Tretyakov, “Polarizabilities of nonreciprocal bianisotropic particles,” *Physical Review Applied*, Vol. 1, No. 3, 034005, 2014.
80. Pfeiffer, C. and A. Grbic, “Bianisotropic metasurfaces for optimal polarization control: Analysis and synthesis,” *Physical Review Applied*, Vol. 2, No. 4, 044011, 2014.
81. Ranjbar, A. and A. Grbic, “Analysis and synthesis of cascaded metasurfaces using wave matrices,” *Physical Review B*, Vol. 95, No. 20, 205114, 2017.
82. Chang, P.-H., C.-Y. Kuo, and R.-L. Chern, “Wave propagation in bianisotropic metamaterials: Angular selective transmission,” *Optics Express*, Vol. 22, No. 21, 25710–25721, 2014.
83. Chern, R.-L. and P.-H. Chang, “Wave propagation in pseudo-chiral media: Generalized Fresnel equations,” *JOSA B*, Vol. 30, No. 3, 552–558, 2013.
84. Dimitriadis, A. I., N. V. Kantartzis, T. D. Tsiboukis, and C. Hafner, “Generalized non-local surface susceptibility model and Fresnel coefficients for the characterization of periodic metafilms with bianisotropic scatterers,” *Journal of Computational Physics*, Vol. 281, 251–268, 2015.
85. Evlyukhin, A. B., V. R. Tuz, V. S. Volkov, and B. N. Chichkov, “Bianisotropy for light trapping in all-dielectric metasurfaces,” *Physical Review B*, Vol. 101, No. 20, 205415, 2020.
86. Furs, A. N., “Surface electromagnetic waves in 1D optically active photonic crystals,” *Journal of Optics*, Vol. 13, No. 5, 055103, 2011.

87. Gauthier, R., "The bianisotropic formulation of the plane wave method from Faraday's and Ampere's Laws," *Optics and Photonics Journal*, Vol. 11, No. 8, 360–386, 2021.
88. Guo, Q., W. Gao, J. Chen, Y. Liu, and S. Zhang, "Line degeneracy and strong spin-orbit coupling of light with bulk bianisotropic metamaterials," *Physical Review Letters*, Vol. 115, No. 6, 067402, 2015.
89. Guo, R.-P., Q.-H. Guo, L.-T. Wu, J. Chen, and D. Fan, "Optical spin-sensitive Zitterbewegung in bianisotropic metamaterials," *Optics Express*, Vol. 24, No. 13, 13788–13799, 2016.
90. Hasar, U. C., J. J. Barroso, T. Karacali, and M. Ertugrul, "Semi-infinite reflection coefficients of bi-anisotropic metamaterial slabs including boundary effects," *IEEE Microwave and Wireless Components Letters*, Vol. 25, No. 5, 283–285, 2015.
91. Karimi, P., B. Rejaei, and A. Khavasi, "Unidirectional surface waves in bi-anisotropic media," *IEEE Journal of Quantum Electronics*, Vol. 54, No. 6, 1–6, 2018.
92. Keller, S. M. and G. P. Carman, "Electromagnetic wave propagation in (bianisotropic) magnetoelectric materials," *Journal of intelligent material systems and structures*, Vol. 24, No. 5, 651–668, 2013.
93. Lunnemann, P., I. Sersic, and A. Femius Koenderink, "Optical properties of two-dimensional magnetoelectric point scattering lattices," *Physical Review B*, Vol. 88, No. 24, 245109, 2013.
94. Mackay, T. G. and A. Lakhtakia, "Negative refraction, negative phase velocity, and counterposition in bianisotropic materials and metamaterials," *Physical Review B*, Vol. 79, No. 23, 235121, 2009.
95. Morgado, T. A., S. I. Maslovski, and M. G. Silveirinha, "Uniaxial indefinite material formed by helical-shaped wires," *New Journal of Physics*, Vol. 14, No. 6, 063002, 2012.
96. Peng, L., Y. Chen, Y. Yang, Z. Wang, F. Yu, G. Wang, N.-H. Shen, B. Zhang, C. M. Soukoulis, and H. Chen, "Spin momentum-locked surface states in metamaterials without topological transition," *Laser & Photonics Reviews*, Vol. 12, No. 8, 1800002, 2018.
97. Peng, L., L. Duan, K. Wang, F. Gao, L. Zhang, G. Wang, Y. Yang, H. Chen, and S. Zhang, "Transverse photon spin of bulk electromagnetic waves in bianisotropic media," *Nature Photonics*, Vol. 13, No. 12, 878–882, 2019.
98. Ra'di, Y. and A. Alù, "Nonreciprocal wavefront manipulation in synthetically moving metagratings," *Photonics*, 2020.
99. Ra'di, Y. and A. Grbic, "Magnet-free nonreciprocal bianisotropic metasurfaces," *Physical Review B*, Vol. 94, No. 19, 195432, 2016.
100. Ranjbar, A. and A. Grbic, "Broadband, multiband, and multifunctional all-dielectric metasurfaces," *Physical Review Applied*, Vol. 11, No. 5, 054066, 2019.
101. Semchenko, I. V., S. A. Khakhomov, S. A. Tretyakov, A. H. Sihvola, and E. A. Fedosenko, "Reflection and transmission by a uniaxially bi-anisotropic slab under normal incidence of plane waves," *Journal of Physics D: Applied Physics*, Vol. 31, No. 19, 2458, 1998.
102. Tretyakov, S. and A. Sochava, "Novel uniaxial bianisotropic materials: Reflection and transmission in planar structures," *Progress In Electromagnetics Research*, Vol. 9, 157–179, 1994.
103. Barkovskii, L. M., G. N. Borzdov, and A. V. Lavrinenko, "Fresnel's reflection and transmission operators for stratified gyroanisotropic media," *Journal of Physics A: Mathematical and General*, Vol. 20, No. 5, 1095, 1987.
104. LaBalle, M. and M. Durach, "Additional waves and additional boundary conditions in local quartic metamaterials," *OSA Continuum*, Vol. 2, No. 1, 17–24, 2019.
105. Durach, M., "Complete 72-parametric classification of surface plasmon polaritons in quartic metamaterials," *OSA Continuum*, Vol. 1, No. 1, 162–169, 2018.
106. Achouri, K. and O. J. Martin, "Surface-wave dispersion retrieval method and synthesis technique for bianisotropic metasurfaces," *Physical Review B*, Vol. 99, No. 15, 155140, 2019.
107. Lunnemann, P. and A. F. Koenderink, "Dispersion of guided modes in two-dimensional split ring lattices," *Physical Review B*, Vol. 90, No. 24, 245416, 2014.
108. Mousvai, S. M., B. A. Arand, and K. Forooraghi, "Surface wave propagation on bianisotropic metasurfaces by using electric and magnetic polarizabilities," *IEEE Access*, Vol. 9, 54241–54253,

- 2021.
109. Popov, V., A. V. Lavrinenko, and A. Novitsky, "Surface waves on multilayer hyperbolic metamaterials: Operator approach to effective medium approximation," *Physical Review B*, Vol. 97, No. 12, 125428, 2018.
  110. Xia, L., B. Yang, Q. Guo, W. Gao, H. Liu, J. Han, W. Zhang, and S. Zhang, "Simultaneous TE and TM designer surface plasmon supported by bianisotropic metamaterials with positive permittivity and permeability," *Nanophotonics*, Vol. 8, No. 8, 1357–1362, 2019.
  111. Yu, Y.-Z., C.-Y. Kuo, R.-L. Chern, and C. T. Chan, "Photonic topological semimetals in bianisotropic metamaterials," *Scientific Reports*, Vol. 9, No. 1, 1–13, 2019.
  112. Darinskii, A., "Surface electromagnetic waves in bianisotropic superlattices and homogeneous media," *Physical Review A*, Vol. 103, No. 3, 033501, 2021.
  113. Darinskii, A., "Surface plasmon polaritons in metal films on anisotropic and bianisotropic substrates," *Physical Review A*, Vol. 104, No. 2, 023507, 2021.
  114. Razzaz, F. and M. A. Alkanhal, "Terahertz evanescent wave tunneling in bianisotropic thin films," *2018 International Applied Computational Electromagnetics Society Symposium (ACES)*, IEEE, 2018.
  115. Razzaz, F. and M. A. Alkanhal, "Electromagnetic tunneling and resonances in pseudo-chiral omega slabs," *Scientific Reports*, Vol. 7, No. 1, 1–9, 2017.
  116. Razzaz, F. and M. A. Alkanhal, "Resonances in bianisotropic layers," *IEEE Photonics Journal*, Vol. 10, No. 1, 1–12, 2017.
  117. Popov, V., A. V. Lavrinenko, and A. Novitsky, "Operator approach to effective medium theory to overcome a breakdown of Maxwell Garnett approximation," *Physical Review B*, Vol. 94, No. 8, 085428, 2016.
  118. Born, M. and E. Wolf, *Principles of Optics: Electromagnetic Theory of Propagation, Interference and Diffraction of Light*, Elsevier, 2013.
  119. Airy, G. B., "VI. On the phenomena of Newton's rings when formed between two transparent substances of different refractive powers," *The London, Edinburgh, and Dublin Philosophical Magazine and Journal of Science*, Vol. 2, No. 7, 20–30, 1833.
  120. Fabry, C. and A. Perot, "Theorie et applications d'une nouvelle methode de spectroscopie interferentielle," *Ann. Chim. Phys.*, Vol. 16, No. 7, 1899.
  121. Perot, A. and C. Fabry, "On the application of interference phenomena to the solution of various problems of spectroscopy and metrology," *Astrophysical Journal*, Vol. 9, 87, 1899.
  122. Kavokin, A. V., J. J. Baumberg, G. Malpuech, and F. P. Laussy, *Microcavities*, Oxford University Press, 2011.
  123. Bozhevolnyi, S. I., *Plasmonic Nanoguides and Circuits*, Pan Stanford Publishing, 2009.
  124. Lindell, I. V., "On the classification of electromagnetic media," *2010 URSI International Symposium on Electromagnetic Theory*, IEEE, 2010.
  125. Graglia, R. D., M. S. Sarto, and P. L. Uslenghi, "TE and TM modes in cylindrical metallic structures filled with bianisotropic material," *IEEE Transactions on Microwave Theory and Techniques*, Vol. 44, No. 8, 1470–1477, 1996.
  126. Lindell, I. V., L. Bergamin, and A. Favaro, "Decomposable medium conditions in four-dimensional representation," *IEEE Transactions on Antennas and Propagation*, Vol. 60, No. 1, 367–376, 2011.
  127. Lindell, I. V. and F. Olyslager, "Generalized decomposition of electromagnetic fields in bianisotropic media," *IEEE Transactions on Antennas and Propagation*, Vol. 46, No. 10, 1584–1585, 1998.
  128. Uslenghi, P. L., "TE-TM decoupling for guided propagation in bianisotropic media," *IEEE Transactions on Antennas and Propagation*, Vol. 45, No. 2, 284–286, 1997.
  129. Durach, M. and A. Rusina, "Transforming Fabry-Perot resonances into a Tamm mode," *Physical Review B*, Vol. 86, No. 23, 235312, 2012.
  130. Keene, D. and M. Durach, "Hyperbolic resonances of metasurface cavities," *Optics Express*, Vol. 23, No. 14, 18577–18588, 2015.



131. Keene, D., M. LePain, and M. Durach, "Ultimately thin metasurface wave plates," *Annalen der Physik*, Vol. 528, Nos. 11–12, 767–777, 2016.
132. Berreman, D. W., "Optics in stratified and anisotropic media:  $4 \times 4$ -matrix formulation," *JOSA*, Vol. 62, No. 4, 502–510, 1972.
133. Hodges, R., C. Dean, and M. Durach, "Optical neutrality: Invisibility without cloaking," *Optics Letters*, Vol. 42, No. 4, 691–694, 2017.
134. D'yakonov, M. I., "New type of electromagnetic wave propagating at an interface," *Sov. Phys. JETP*, Vol. 67, No. 4, 714–716, 1988.
135. Takayama, O., L.-C. Crasovan, S. K. Johansen, D. Mihalache, D. Artigas, and L. Torner, "Dyakonov surface waves: A review," *Electromagnetics*, Vol. 28, No. 3, 126–145, 2008.
136. Takayama, O., L. Crasovan, D. Artigas, and L. Torner, "Observation of Dyakonov surface waves," *Physical Review Letters*, Vol. 102, No. 4, 043903, 2009.
137. Takayama, O., D. Artigas, and L. Torner, "Practical dyakonons," *Optics Letters*, Vol. 37, No. 20, 4311–4313, 2012.
138. Polo, J., T. Mackay, and A. Lakhtakia, *Electromagnetic Surface Waves: A Modern Perspective*, Newnes, 2013.